Proc. Natl. Acad. Sci. USA
Vol. 78, No. 3, pp. 1341–1345, March 1981
Biochemistry

Systematic punctuation of eukaryotic DNA by A+T-rich sequences

(genome structure/partial DNA denaturation/electron microscopy)

JACQUES MOREAU, LUDMILLA MATYASH-SMIRNIAGUINA, AND KLAUS SCHERRER

Service de Biochimie de la Différenciation, Institut de Recherche en Biologie Moléculaire, 75251 Paris, Cedex 05 France

Communicated by Robert Palese Perry, September 19, 1980

ABSTRACT **Isodenaturation of avian and mammalian DNA of $M_r > 2.5 \times 10^8$ in 85% (vol/vol) formamide led to the observation by electron microscopy of A+T-rich zones ("AT-rich linkers") of 300–3000 base pairs which are distributed over the entire genome in a characteristic pattern. Linkers of mean length 800 base pairs are found either isolated or in clusters of about four to six linkers of more heterogeneous size separated on average by 2500 base pairs (in duck DNA). In between clusters, single linkers segment the DNA at distances of 10 to more than 100 kilobase pairs, with a majority in the range of 10–30 kilobase pairs. An analogous organization of linkers is found in rat and mouse DNA. The internal organization of the clusters varies, however, in a fashion that might be related to the large amount of light satellite DNA in the mouse and its apparent absence in rat and avian DNA. It is possible to fragment the DNA under appropriate conditions by the single-strand-specific nuclease S1 at the site of these A+T-rich zones and to obtain, on alkaline sucrose gradients, a bimodal pattern of DNA fragments of the size corresponding to the pattern observed by electron microscopy. The implications of this observation for DNA organization, chromatin structure, units of transcription and replication, and possible targets of A+T-specific drugs are discussed.**

Although abundant data are available concerning general characteristics of eukaryotic DNA and although knowledge of detailed DNA sequence organization is rapidly proliferating (see ref. 1 for a review), relatively little is known about genome architecture at intermediate levels of resolution. In particular, no features in DNA are known that would permit the definition of functional units involved in, e.g., replication, transcription, or the chromosome architecture underlying the well-known morphological patterns in polytene or lampbrush chromosomes or those found recently in metaphase (2) or interphase (3, 4) chromosomes of higher organisms.

The significance of the large excess of transcribed and untranscribed genomic DNA, compared to the complexity of the actual translated mRNA, is enigmatic, although the final confirmation of the existence of precursors to mRNA allows at least a tentative interpretation of the existence of transcribed nongenic DNA within the eukaryotic transcriptons (see discussion and references in ref. 5). Light satellite DNA (6–10) is an example of nontranscribed (9), probably structural, DNA. Further A+T-rich segments disseminated in eukaryotic DNA (11) might play an important role in DNA structure and function (see model for precursor mRNA in ref. 12) beyond their enrichment at the centromere (10) of metaphase chromosomes. A+T-rich DNA sequences have been found in bacterial promoter/operator regions (13, 14) and in gene-proximal eukaryotic spacers (15). Such sequences are possible targets of A+T-specific drugs such as distamycin or bromodeoxyuridine, which interfere, respectively, with transcription (16) and specific phases of differentiation (17).

The publication costs of this article were defrayed in part by page charge payment. This article must therefore be hereby marked "*advertisement*" in accordance with 18 U. S. C. §1734 solely to indicate this fact.

We thus set out to study the distribution and characteristics of A+T-rich regions in segments of eukaryotic DNA longer than the putative transcriptional units defined by the size of the transcription products (for discussion, see ref. 5).

METHODS

DNA Preparation. Erythroblasts were selected from the blood of anemic Pekin ducks and were washed in 10 mM Tris·HCl, pH 6.9/10 mM KCl/3 mM $MgCl_2$/1 mM $MnCl_2$/0.25 M sucrose. The cells were lysed with 0.4% Cemusol NP-6 in washing buffer (pH 7.4) in a precision-bore, hydraulically driven Dounce homogenizer. Nuclei were washed with a double detergent solution (0.5% Tween/0.15% deoxycholate) for 10 sec, diluted with 10 vol of washing buffer, resuspended in 10 mM Tris·HCl, pH 7.4/150 mM NaCl, lysed by 0.5% $NaDodSO_4$, gently transferred to a dialysis bag, and incubated overnight at 18°C with proteinase K (50 μg/ml) in 5 mM EDTA. Protein was removed by extraction in slow-motion roller bottles (18) first with saturated phenol, then with phenol/chloroform/isoamyl alcohol, 1:1:0.02 (vol/vol), and finally with chloroform. DNA was then dialyzed against 10 mM NaCl/50 mM Tris·HCl/1 mM EDTA, treated with pancreatic RNase (1 mg/150 ml for 3 hr at 20°C), extracted with satured phenol, and dialyzed exhaustively against Tris·HCl, pH 7.8/100 mM NaCl/1 mM EDTA. Rat and mouse liver cell suspensions were treated similarly.

Electron Microscopy. Denatured regions in DNA were seen by electron microscopy by the isodenaturation procedure (19). DNA (0.5 μg/ml) in 0.1 M Tris·HCl, pH 7.8/10 mM EDTA with various concentrations of formamide (repurified) was spread, after addition of cytochrome to 40 μg/ml, on a hypophase containing the same buffer diluted 1:10 and a formamide concentration 30% lower than that in the hyperphase. Protein films were transferred to 200-mesh grids covered by Parlodion. After the grids were dipped in 90% ethanol, they were stained with uranyl acetate and shadowed with palladium platinum by rotation at an angle of 6° or 7°. The grids were observed at 4000- or 6000-fold primary magnification in a Siemens Elmiscope 101 operating at 80 kV. Final magnification was determined by grating replica (54,800 lines/inch), and DNA molecules were measured on positives by a digitizer branched on a HP 9830 calculator. The measuring error was determined to less than ±5% on the shortest elements measured.

Nuclease S1 Treatment. Nuclease S1 (3–4 units/μg of DNA) from *Aspergillus oryzae* (EC 3.1.30.1; Sigma type III) was added to a solution of DNA dialyzed against twice concentrated buffer; 1 vol of formamide was then added. Incubation was for 2½ hr in 30 mM sodium acetate, pH 6/50 mM NaCl/1 mM Zn^{2+}/5% (wt/vol) glycerol/50% (vol/vol) formamide. The reaction was arrested by addition of EDTA and Tris (pH 7.8) to 5 mM and 25 mM, respectively.

Abbreviations: bp, base pairs; kbp, kilobase pairs.

RESULTS

The sedimentation characteristics of the DNA prepared relative to those of T4 or λ phage DNA markers showed that molecules of $M_r > 250 \times 10^6$ (380 kbp) were obtained including, hence, several putative transcriptions (5).

In order to define the conditions for isodenaturation of DNA segments of high A+R content, the melting of linear plasmid pBR322 DNA cut with restriction enzyme *Pst* I was analyzed. This DNA includes a more centrally located stretch of 360 base pairs (bp) with 62% A+T content and a peripherally located (10.64%) 100 bp of 74% A+T content. These were fully stable at 85% formamide, but they started to melt at 90% formamide (Fig. 1*C*). Out of 540 molecules observed by electron microscopy, 37.2% showed a single bubble, located between 8% and 13% at one extremity, if spread in 90% formamide at 23°C under the conditions specified in *Methods*. A change in melting temperature (Δt_m) of 0.55°C/1% of formamide was calculated, close to that given by Tibbetts *et al.* (20). This value and the t_m derived in H_2O buffer from the base composition (21) allow us to calculate that random p(dA-dT) would melt in 67% formamide and that duck DNA [average sequence, 56% A+T (22)] would melt in 100% formamide. An analogous calculation shows that DNA that denatured in 85% formamide must contain at least 80% A+T.

A further problem was to determine the length of DNA molecules under our conditions appropriate to serve as molecular weight standards, allowing us to convert electron microscopic measurements to molecular weight with appropriate precision. We chose *Eco*RI-treated pBR322 DNA (4360 bp) and phage λ DNA (50,000 bp), which were spread and measured by electron microscopy. These standard molecules contained 3125 bases per μm, with a standard deviation of 0.020. To determine the analogous value for single-stranded DNA, we measured phage φX174 DNA and found it to be 3980 bases per μm.

Detection by Electron Microscopy of A+T Rich Segments in Duck DNA Spread Under Conditions of Limited Denaturation. Under the conditions adopted, there was no denaturation of DNA segments at concentrations below 50% formamide. However, some rare, fully single-stranded regions of more than 5 kbp were present. No replication forks were observed. Between 50% and 75% formamide, no characteristic denaturation

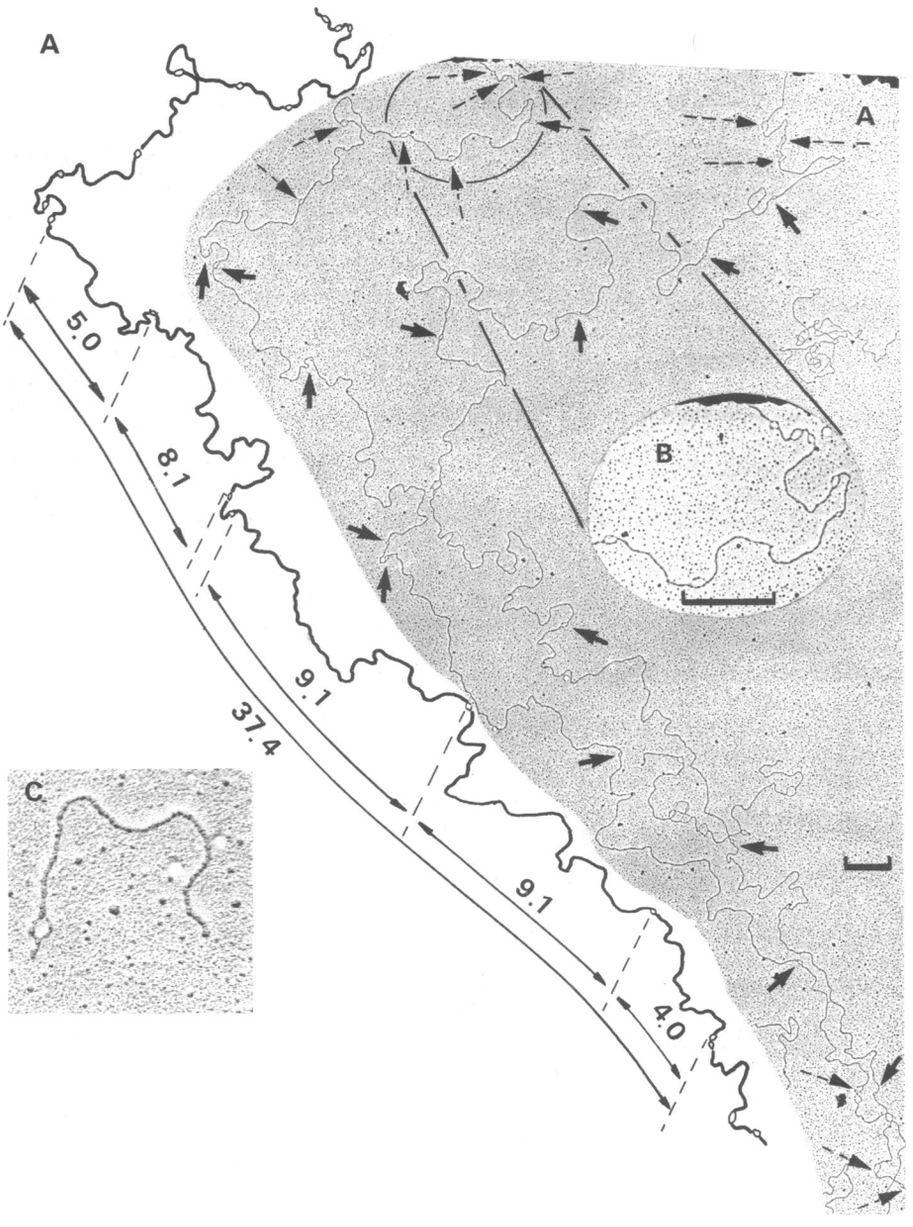

FIG. 1. Electron micrographs of isodenatured duck DNA molecules. (*A*) Micrograph and graphic representation of continuous DNA molecules denatured by 85% formamide, showing clusters (broken arrows) and individual regions (thick arrows) of partial denaturation. (*B*) Same as *A* but higher magnification of a DNA section containing A+T-rich denatured regions. (*C*) Isodenaturation of a 100-bp A+T-rich (74% A+T) segment in a pBR322 linearized DNA molecule exposed to 90% formamide. (Bar = 1 μm.)

pattern can be observed in homogeneous DNA molecules up to 200 μm long (up to 620 kbp). Over this entire concentration range, we again found the rare, fully single-stranded DNA molecules that were more than 5 kbp long. We do not know the significance of this phenomenon. The existence of single-stranded DNA in preparations of eukaryotic DNA has been reported (23); the structures we observe may correspond to *a priori* single-stranded DNA.

Between 75% and 85% formamide, "bubbles" of denaturation of the type shown in Figs. 1 and 2, appeared within the spread DNA. These DNA segments must contain ≈80% A+T. At 85% formamide a threshold level is reached. Indeed, in duck DNA (Figs. 1 and 3*A*), the number of denatured regions of uniform size is maximal under these conditions; at concentrations greater than 90% formamide, random denaturation of longer DNA segments starts (not shown). The occurrence of these bubbles is a general phenomenon. We have examined more than 200 grids so far, and we have not detected any DNA molecules that were 100–300 kbp long and devoid of these zones that denatured prior to random-sequence eukaryotic DNA.

Analysis of the electron micrographs indicated that the size and distribution of the A+T-rich denatured DNA segments shown in Fig. 1*A* follow a characteristic pattern. The small bubbles occur either isolated (Fig. 1*A*, thick arrows) or else in clusters, with several of them in a row (Fig. 1*A*, broken arrows). We refer to these denatured structures as "AT-rich linkers" because they seem to link segments of the random-sequence DNA.

The size distribution of such linkers is relatively narrow. Fig. 3*A* shows the histogram obtained when the length of single-stranded duck DNA was measured in between two areas not denatured in 85% formamide. Their range was 0.1–1.0 μm, corresponding to 0.3–3.1 kb, with a first modal peak at 0.2 μm, corresponding to about 800 bases in a row.

Measuring the length of the DNA segments in between linkers, we found a characteristic distribution of very long segments of undenatured DNA and of relatively short segments, which very likely corresponds to the stable DNA segments inside and outside the clusters. Fig. 4 shows the histograms of this distribution. In order to evaluate the true mass distribution of DNA, the numbers of molecules represented were multiplied by the corresponding molecular weight. About 70% by number of the intact DNA segments are less than 3.5 μm long, and two-thirds of these are less than 1.5 μm, with possible modes at 0.3 μm and 0.8 μm (Fig. 4). These modes correspond to about 1.0 and 2.5 kbp, based on a conversion factor of 3125 bp/μm. The mean length of these relatively short stable segments up to 2.5 μm is calculated to be 0.8 μm or 2600 bp. These short sections may correspond mainly to the DNA found within the clusters. On the other hand, 30% of the fragments by number (64% of the measured DNA length) fall into a wide range of lengths of between 3.5 μm to more than 40 μm (10–125 kpb); of these, most fall into a more narrow range of 3.5–9.5 μm or 11–30 kbp. This size class includes the sections of the DNA seen outside the clusters. However, these size classes overlap; the only firm observation relates to the clustering of linkers in some areas.

An organizational pattern often encountered in electron micrographs of DNA spread in 85% formamide consists of repeated DNA segments delimited by two clusters of multiple A+T-rich zones. In measurements of nine DNA stretches longer than 50 μm, the average length of the repeated segment was 33.5 μm (104.4 kbp), the framing clusters (linkers plus internal DNA) were 7.8 μm (24.4 kbp), and the segments within the frame were on the average 25.6 μm (80 kbp). Single linkers further segmented the latter segments into fractions of on av-

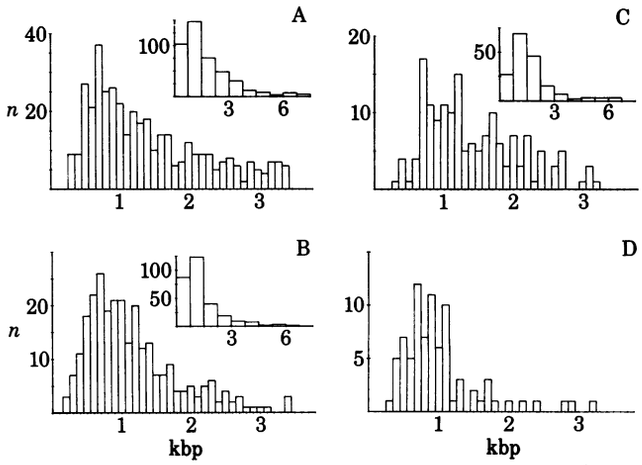

FIG. 3. Length histogram of denatured regions in 85% formamide. The following DNAs were denatured (the number of molecules measured is given in parentheses): (*A*) duck DNA (440); (*B*) mouse DNA (250); (*C*) rat DNA (180); (*D*) as in *A* but clusters were omitted and isolated linkers were measured exclusively (80).

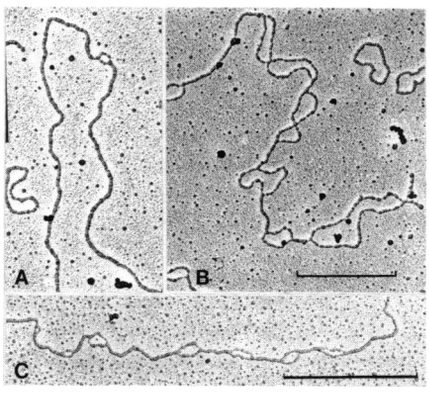

FIG. 2. Electron micrograph of mammalian DNA denatured in 85% formamide. DNA molecules were denatured as described in the legend for Fig. 1. Mouse DNA: (*A*) isolated linker 500 bp long; (*B*) cluster with typically fused linkers (such regions easily break open; circular molecules are plasmid pBR322 DNA). Rat DNA: (*C*) Individual linkers at relatively short distances.

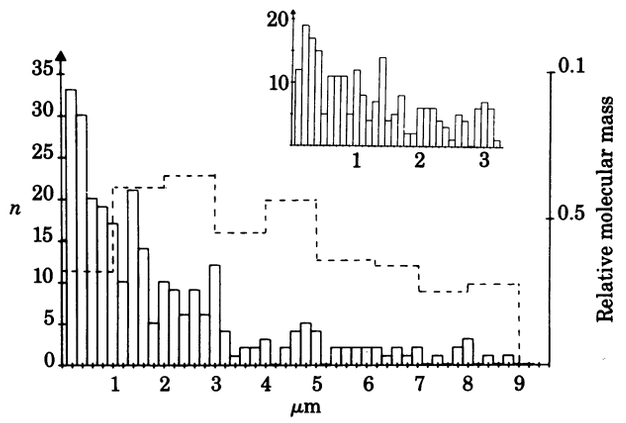

FIG. 4. Length histogram of uninterrupted double-stranded DNA in between regions that isodenatured in 85% formamide. The broken line represents the distribution of relative DNA mass given by multiplication of the number of molecules by the DNA length in any given size class.

erage 6.3 μm (20.7 kbp). The shortest segment outside the clusters within these nine repeated sequences measured was 7.8 kbp, and the longest was 58.7 kbp; the average number of linkers in a cluster was four to six. Fig. 1*A* may thus illustrate the major part of such a repetitive superstructure.

A+T-Rich Linkers in Mammalian DNA. Confronted with the question of whether this feature was specific to avian DNA or was, rather, a general element of the eukaryotic genome structure, and in view of the surprising difference in amount of light satellite DNA in these otherwise closely related species, we chose to analyze rate and mouse DNA. We hoped that we might be able to conclude whether the linker structure is related to the light satellite DNA, abundant in mouse but largely absent in rat and avian DNA.

In rat and mouse DNA spread under conditions identical to those applied to duck DNA (85% formamide) we observed the characteristic linkers in a pattern similar to that analyzed for duck DNA (Fig. 1*A*): A+T-rich linkers were either isolated (Fig. 2*A*) or organized into clusters (Fig. 2 *B* and *C*). As in the duck genome, the phenomenon was general; we found no DNA stretches longer than 100 kbp without such linkers.

Fig. 3 gives the histograms of the single-strand length of the denatured linkers in duck (Fig. 3*A*), mouse (Fig. 3*B*), and rat (Fig. 3*C*) DNA. The most striking observation concerns the similarity of the three histograms. In all three, a first modal peak at a DNA length of less than 1000 bp was observed. In mouse DNA it was localized between 600 and 1000 bp; in rat DNA, between 700 and 1200 bp, and in duck DNA, between 500 and 1000 bp. The first modal length of about 800 bp very likely corresponds to the linkers outside the clusters. Indeed, if the analysis is restricted to isolated linkers, the histogram (Fig. 3*D*) shows a much more narrow size distribution of about 800 bp (in duck).

In a random analysis of isolated and clustered linkers, the mean length determined in DNA of mouse, rat, and duck was 1323, 1427, and 1413 bp, respectively, if measurements up to 3.5 kbp were taken into account, or 1540, 1690, and 1709 bp, respectively, if denaturations up to 7.0 kbp were measured. These determinations give a standard mean length of about 1400 bp (or 1600 bp) for the linkers in all three species.

A qualitative observation, hard to quantitate, singles out the mouse linkers compared to those observed in the other two species. In mouse DNA, the linkers in clusters were often "fused," as shown in Fig. 2*B*; in the two other species, the linkers were in general well separated even in clusters (compare Figs. 1 and 2*C*). It is possible that this feature drains (for mouse) relatively more DNA into the light satellite peak. Further work will be necessary to establish or refute this interpretation. However, the data presented here demonstrate that the basic organization of A+T-rich linkers shown for duck in Fig. 1 applies to mammalian DNA as well.

Enzymatic Fragmentation of Duck DNA at the Level of A+T-Rich Segments. Corroboration of the data reported above was obtained by an entirely different experimental approach, which enabled us to fragment the duck DNA preferentially at the level of the A+T-rich linkers with a single-strand-specific nuclease. We took advantage of the preferential "breathing" of such A+T-rich segments under thermodynamic conditions where the random-sequence DNA would remain perfectly stable. Duck DNA of M_r >250 × 10^6 was efficiently cut by nuclease S1 of *A. oryzae*.

At pH 4.5, optimal for nuclease S1, hydrogen bonds are slightly destabilized. Indeed, at low pH and relatively low concentration, extensive fragmentation of DNA takes place in the absence of any enzyme (not shown). It is not excluded that such breakage takes place precisely and preferentially at the level of the A+T-rich zones, which represent "weak spots" in the DNA structure. As a compromise we chose to treat DNA at pH 6, which gave 10–20% of maximal enzyme activity. To slightly destabilize DNA, we adopted an 80 mM Na^+ buffer in 50% formamide; the nuclease was still partially active under such conditions (24) and spontaneous fragmentation was reduced to tolerable levels (see control in Fig. 5). Incubation was at 27°C for 1–2.5 hr; we found that net DNA hydrolysis was below 7% and did not increase significantly during this time.

Alkaline sucrose gradient analysis (Fig. 5) of such enzymatically fragmented DNA showed a striking, essentially bimodal, distribution of the resulting fragments. The major component sedimented in a molecular weight zone delimited by a T4 phage DNA marker (M_r 105 × 10^6, 160 kbp) and extending down to a single-strand M_r of ≈ 5 × 10^6 (15 kbp), with a mode corresponding to M_r 11–14 × 10^6 or 33–42 kbp. About 10% of the DNA sedimented as small fragments in a distribution corresponding to a mean M_r of 0.8 × 10^6 or 2.5 kbp (determined in pooled fractions; note that the very last "peak" is background in part due to the gradient-expulsion buffer interphase). Furthermore, we regularly observed a heavy shoulder on the peak formed by the light DNA.

Control experiments demonstrated that DNA fragmentation under our conditions is due to the presence of the enzyme. The sedimentation pattern of the control DNA carried through the procedure without addition of enzyme (Fig. 5) showed, in addition to fragments of M_r > 50 × 10^6 (single strand), a small amount of the components obtained by nuclease cleavage. One might thus suggest that the A+T-rich linkers are, as expected, weak spots, allowing for preferential breakage of the DNA. Due to the breathing phenomenon another obvious control, "random" cleavage of DNA with nuclease under "nondenaturing" conditions, is meaningless: the enzyme will, under any condition, attack the A+T-rich zones first.

As a main conclusion to be drawn from these experiments, exposure to a single-strand-specific nuclease acting under conditions of DNA "breathing" does not yield randomly fragmented DNA but leads to a characteristic bimodal distribution of fragments. Of those, 25%, representing 90% of the DNA mass, were found in the 15- to 150-kbp range; 75% of the number of fragments (10% of the DNA mass) were found in molecules of on average 5 kbp. Comparing these figures to those

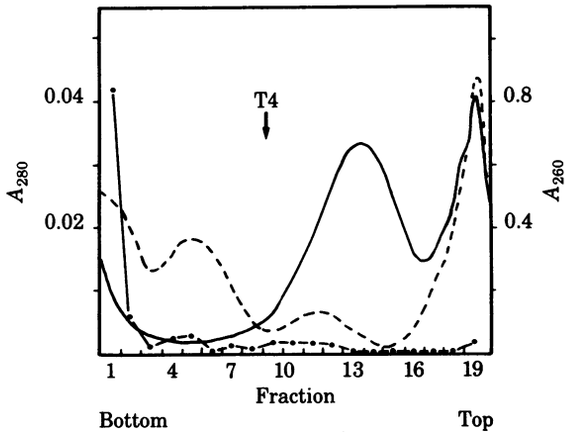

FIG. 5. Alkaline sucrose gradient analysis of DNA fragmented by nuclease S1. About 0.3 A_{254} unit of DNA was placed on isokinetic alkaline sucrose gradients (15–29% sucrose in 0.1 M NaOH/0.9 M NaCl) and centrifuged (Beckman SW 41 rotor, 18 hr, 4°C, 20,000 rpm). —·— (A_{260}), Native DNA (hand-collected from the top); ——, DNA fragmented by nuclease S1; -------, control DNA incubated in the absence of enzyme. The arrow gives the position of T4 phage DNA (160 kbp) molecular weight marker that was sedimented on a parallel gradient.

obtained by the denaturation experiments, we tentatively conclude that we have, indeed, succeeded in partially fragmenting the DNA at the level of the A+T-rich linkers observed by electron microscopy. Partial denaturation and nuclease S1 cleavage thus reveal a similar pattern of duck DNA subunit structure delimited by the A+T-rich linkers.

DISCUSSION

Our main result is the discovery of a general structural feature of eukaryotic DNA which may amount to a systematic subdivision and punctuation of the DNA molecule. This feature may prove helpful in comprehending the internal organization of DNA and the function of its noncoding segments. There is no room here to discuss at length all aspects of our observations. Our preliminary work (not shown) shows that avian globin genes are localized in DNA segments larger than 7 kbp. Furthermore, *Drosophila* DNA contains the same type of A+T-rich linkers. Because the genetically mapped *Drosophila* polytene chromosome bands represent one of the rare cases of clearly defined eukaryotic transcriptons, we set out to map the linkers in relation to a specific gene. It is not excluded that such linkers might correlate with features framing and defining transcriptional units. Indeed, the distances separating single linkers outside clusters correlate well with the size of the bulk primary transcripts in eukaryotic cells (see discussion in ref. 5).

The existence of A+T-rich zones with a G+C content even lower than that reported for mammalian and avian light satellite DNA (≈60–65%) seems to be real and a general feature of eukaryotic DNA. They are found in mitochondrial DNA of yeast (25), particularly in petite mutants (26), but they are also found in mammalian DNA. Indeed, while our investigations proceeded, Vizard *et al.* (27) showed that, after exposure to 85% formamide, 1750-bp denatured zones were widely distributed over human DNA. Their further measurements, however, cannot be easily correlated with ours because much shorter DNA molecules than those prepared for our present study were analyzed. Indeed, our most striking observation is the bimodal arrangements of the A+T-rich linkers either in clusters or singly, interrupting the DNA only at considerable distances. Recent DNA sequence data revealed A+T-rich zones in defined positions relative to coding sequences. Actin genes in *Dictyostelium* are literally embedded in almost pure A+T-rich DNA (28); Lazowska *et al.* (29) found a 656-bp A+T-rich spacer within the first intervening sequence of the cytochrome *b* gene of yeast mitochondria.

The data obtained here indicate that the pattern of A+T-rich linkers provides for a significant subdivision of the eukaryotic DNA, which ultimately must be related to some function. A+T-rich DNA devoid of coding information may be related to "punctuation" in DNA. Such punctuation in the genome may have arisen as a consequence of evolutionary pressure independent of the coding message but related to genome architecture and function and to chromosome function in mitotic division and meiotic recombination (30). Mouse pachytene DNA is naturally fragmented in a bimodal pattern almost identical to that shown in Fig. 5 (see figure 2 in ref. 31). A+T-type punctuation is probably not restricted to large areas such as the light satellite DNA and the 800-bp linkers, which most likely are located outside the transcriptons. Shorter A+T-rich segments might provide signals for processing of primary precursor to mRNA as they do, e.g., for the precursor to rRNA in *Drosophila* (32); they might define at the 3'-end of the secondary processing products sites for polyadenylylation (12), as demonstrated for adenovirus late transcripts (33). Intragenic and extragenic punctuation is a theoretical necessity in genome organization, and the feature described in this paper, providing easily identifiable landmarks in the otherwise hidden DNA organization, may eventually allow some insight into such a system.

We thank Dr. L. Benedetti of our Institute for introducing one of us (J.M.) to electron microscopy and for hospitality in his laboratory. We thank Kinsey Maundrell for critical reading of the manuscript and R. Scharzmann, O. Champion, and C. Sagot for assistance in its preparation. L.M.-S. is on leave of absence from the Institute of Genetics and Selection of Industrial Microorganisms, Moscow. This investigation was supported by the French Centre National de la Recherche Scientifique, Institut National de la Santé et da la Recherche Médicale, and the Foundation pour la Recherche Médicale.

1. Ilyin, Y. V. & Georgiev, G. P. (1980) *Crit. Rev. Biochem.* **9**, 250–300.
2. Paulson, J. R. & Laemmli, U. K. (1977) *Cell* **12**, 817–828.
3. Hancock, R., Hugues, M. & Wunderli, H. (1979) *Experientia* **35**, 985.
4. Marsden, M. P. F. & Laemmli, U. K. (1979) *Cell* **17**, 849–858.
5. Scherrer, K., Imaizumi-Scherrer, M. T., Reynaud, C. A. & Therwath, A. (1979) *Mol. Biol. Rep.* **5**, 5–28.
6. Lewin, B. (1974) in *Gene Expression* (Wiley, New York), Vol. 2, p. 148.
7. Pech, M., Igo-Kemenes, T. & Zachau, H. G. (1979) *Nucleic Acids Res.* **7**, 417–432.
8. Thiery, J. P., Macaya, G. & Bernardi, G. (1976) *J. Mol. Biol.* **108**, 219–235.
9. Flamm, W. G., Walker, P. M. B. & McCallum, M. (1969) *J. Mol. Biol.* **40**, 423–443.
10. Pardue, M. L. & Gall, J. G. (1970) *Science* **168**, 1356–1358.
11. Scherrer, K. (1971) *FEBS Lett.* **17**, 68–72.
12. Scherrer, K. (1974) in *Control of Gene Expression*, Advances in Experimental Medicine and Biology, eds. Kohn, A. & Shakey, A. (Plenum, New York), Vol. 44, pp. 169–219.
13. Pribnow, D. (1975) *Proc. Natl. Acad. Sci. USA* **72**, 784–788.
14. Nakamura, K. & Inouye, M. (1979) *Cell* **18**, 1109–1117.
15. Fedoroff, N. V. & Brown, D. D. (1978) *Cell* **13**, 701–716.
16. Zimmer, C. (1975) *Prog. Nucleic Acid Res. Mol. Biol.* **15**, 285–318.
17. Holtzer, H., Rubinstein, N., Fellini, S., Yeoh, G., Chi, J., Birnbaum, J. & Okoyama, M. (1975) *Q. Rev. Biophys.* **8**, 523–557.
18. Gross-Bellard, M., Oudet, P. & Chambon, P. (1973) *Eur. J. Biochem.* **36**, 32–38.
19. Davis, R. W. & Hyman, R. W. (1971) *J. Mol. Biol.* **62**, 287–301.
20. Tibbetts, C., Johanson, K. & Philipson, L. (1973) *J. Virol.* **12**, 218–225.
21. Schildkraut, C. & Lifson, S. (1965) *Biopolymers* **3**, 195–208.
22. Bruns, G. P., Fisher, S. & Lowy, B. A. (1965) *Biochim. Biophys. Acta* **95**, 280–290.
23. Leibovitch, S. A., Leibovitch, M.-P., Kruh, J. & Harel, J. (1979) *Eur. J. Biochem.* **97**, 327–333.
24. Hutton, J. R. & Wetmur, J. G. (1975) *Biochem. Biophys. Res. Commun.* **66**, 942–948.
25. Prunell, A. & Bernardi, G. (1974) *J. Mol. Biol.* **86**, 825–841.
26. Bernardi, G. (1979) *Trend Biochem. Sci.* **4**, 197–201.
27. Vizard, D. L., Rinehart, F. P., Rubin, C. M. & Schmid, C. W. (1977) *Nucleic Acids Res.* **4**, 3753–3768.
28. Firtel, R. A., Timm, R., Kimmel, A. R. & McKeown, M. (1979) *Proc. Natl. Acad. Sci. USA* **76**, 6206–6210.
29. Lazowska, J., Jacq, C. & Slonimski, P. P. (1980) *Cell* **22**, 333–348.
30. Scherrer, K. (1980) in *Eukaryotic Gene Regulation - 1*, ed. Kolodny, L. G. M. (CRC, Boca Raton, FL), pp. 40–100.
31. Hotta, Y., Chandley, A. C. & Stern, H. (1977) *Chromosoma* **62**, 255–268.
32. Pavlakis, G., Jordan, B. R., Wurst, R. M. & Vournakis, S. N. (1979) *Nucleic Acids Res.* **7**, 2213–2238.
33. Nevins, J. R. & Darnell, J. E., Jr. (1978) *Cell* **15**, 1477–1493.